CHEMISTRY
AN ASIAN JOURNAL

DOI: 10.1002/asia.201100979

Dithienocyclopentathieno[3,2-*b*]thiophene Hexacyclic Arene for Solution-Processed Organic Field-Effect Transistors and Photovoltaic Applications

Yen-Ju Cheng,* Chiu-Hsiang Chen, Tai-Yen Lin, and Chain-Shu Hsu*[a]

Abstract: We have developed a ladder-type dithienocyclopentathieno[3,2-*b*]thiophene (**DTCTT**) hexacyclic unit in which the central thieno[3,2-*b*]thiophene ring was covalently fastened to two adjacent thiophene rings through carbon bridges, thereby forming two connected cyclopentadithiophene (**CPDT**) units in a hexacyclic coplanar structure. This stannylated **Sn-DTCTT** building block was copolymerized with three electron-deficient acceptors, dibromo-thieno[3,4-*c*]pyrrole-4,6-dione (**TPD**), dibromo-benzothiadiazole (**BT**), and dibromo-phenanthrenequinoxaline (**PQX**), by Stille polymerization, thereby furnishing a new class of alternating donor–acceptor copolymers: **PDTCTTTPD**, **PDTCTTBT**, and **PDTCTTPQX**, respectively. Field-effect transistors based on **PDTCTTPQX** and **PDTCTTBT** yielded high hole mobilities of 0.017 and 0.053 $cm^2 V^{-1} s^{-1}$, respectively, which are among the highest performances among amorphous donor–acceptor copolymers. A bulk heterojunction solar cell that incorporated **PDTCTTTPD** with the lower-lying HOMO energy level delivered a higher V_{oc} value of 0.72 V and a power conversion efficiency (PCE) value of 2.59%.

Keywords: copolymerization · field-effect transistors · photovoltaics · polymers · solar cells

Introduction

Polymer-based organic photovoltaics (OPVs) have attracted considerable interest in the formation of low-cost, lightweight, large-area, and flexible photovoltaic devices.[1] To achieve high efficiencies of these OPVs, the most-difficult challenge is to develop p-type conjugated polymers that simultaneously possess low band-gaps (LBGs), to capture more solar photons, and high hole mobilities for efficient charge-transport. The most-powerful way to prepare a LBG polymer is to link electron-rich-donor- and electron-deficient-acceptor units along the conjugated polymer backbone.[2] Based on this molecular strategy, a large amount of research has been directed towards developing new electron-rich donor segments for p-type materials.[3] Multifused arenes with forced structural planarity have been a common structural feature in donor segments of successful LBG polymers.[3] Forced planarization by covalently fastening adjacent aromatic units into the polymeric backbone provides an effective way to reduce the band-gap, because parallel p-orbital interactions can facilitate π-electron delocalization and elongate the effective conjugation length.[4] Furthermore, rigidification prevents the rotational disorder around interannular single bonds to lower the reorganization energy, which can enhance the intrinsic charge mobility.[5] 4H-cyclopenta[2,1-*b*:3,4-*b*′]dithiophene (**CPDT**)[6] is a tricyclic coplanar thiophene-based unit that has been widely employed as a building block for producing LBG polymers. Poly[2,6-(4,4-bis(2-ethylhexyl)-4H-cyclopenta[2,1-*b*;3,4-*b*′]dithiophene)-*alt*-4,7-(2,1,3-benzothiadiazole)] (**PCPDTBT**), which uses **CPDT** as the donor and **BT** as the acceptor, was one of the first successful LBG polymers to be used in OPVs,[7] and showed very high short-circuit currents (J_{sc}). On the other hand, thieno[3,2-*b*]thiophene is another attractive unit in the fused-thiophene family. The incorporation of symmetrical and coplanar thieno[3,2-*b*]thiophene units into conjugated polymers has been shown to facilitate strong interchain interactions for ordered packing. In addition, thieno[3,2-*b*]thiophene-based conjugated polymers have shown lower-lying HOMO energy levels, which is an important prerequisite for acquiring open-circuit voltage (V_{oc}) values.[8] To improve the solubility of the resulting polymers, it is usually necessary to introduce alkyl chains into the β-positions of the thieno[3,2-*b*]thiophene unit.[8] However, this substitution also has a negative effect on the effective conjugation owing to severe steric-hindrance-induced twisting between neighboring units.[9] By taking these aforementioned points into account, it is of great interest to integrate **CPDT** and thieno[3,2-*b*]thiophene units into a molecular entity with forced rigidification, to simultaneously extend the conjugation, whilst maintaining the coplanarity. Herein, we report a ladder-type dithienocyclopentathieno[3,2-*b*]thiophene (**DTCTT**) unit where the central thieno[3,2-*b*]thiophene ring is covalently fastened to two adjacent thiophene rings through carbon bridges. In views of structural composition, this hexacyclic arene consists of two **CPDT** rings that

[a] Prof. Dr. Y.-J. Cheng, C.-H. Chen, T.-Y. Lin, Prof. Dr. C.-S. Hsu
Department of Applied Chemistry
National Chiao Tung University
1001 Ta Hsueh Road, Hsin-Chu, 30010 (Taiwan)
E-mail: yjcheng@mail.nctu.edu.tw
cshsu@mail.nctu.edu.tw

Supporting information for this article is available on the WWW under http://dx.doi.org/10.1002/asia.201100979.

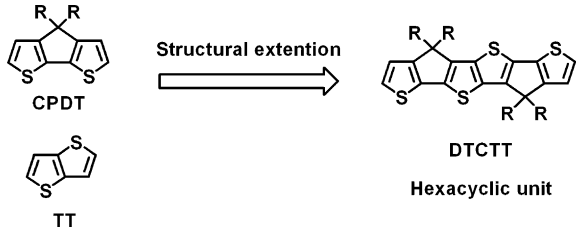

Scheme 1. The chemical structures of the bicyclic (**TT**), tricyclic (**CPDT**), and hexacyclic (**DTCTT**) units.

are connected through a thieno[3,2-*b*]thiophene ring (Scheme 1).

Functionalization at the bridging carbon allows for the introduction of four highly solubilizing side-chains on the two **CP** moieties, thereby making **DTCTT** derivatives highly soluble. Herein, we report the synthesis of a **Sn-DTCTT** monomer that was copolymerized with 1,3-dibromo-5-octylthieno[3,4-*c*]pyrrole-4,6-dione (**TPD**), 2,7-dibromo-2,1,3-benzothiadiazole (**BT**), and 5,8-dibromophenanthrene-quinoxaline (**PQX**) acceptors to afford a new class of conjugated D–A alternating copolymers (Scheme 2). Their thermal, optical, and electrochemical properties have been carefully characterized. These polymers showed promise for applications in solution-processed field-effect transistors and in solar-cell devices.

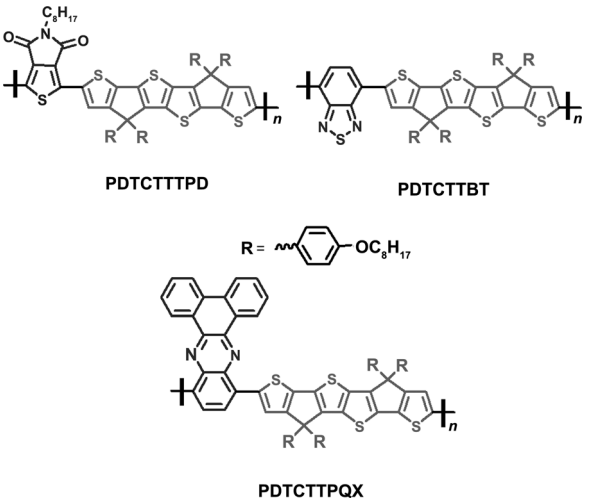

Scheme 2. The chemical structures of polymers **PDTCTTTPD**, **PDTCTTBT**, and **PDTCTTPQX**.

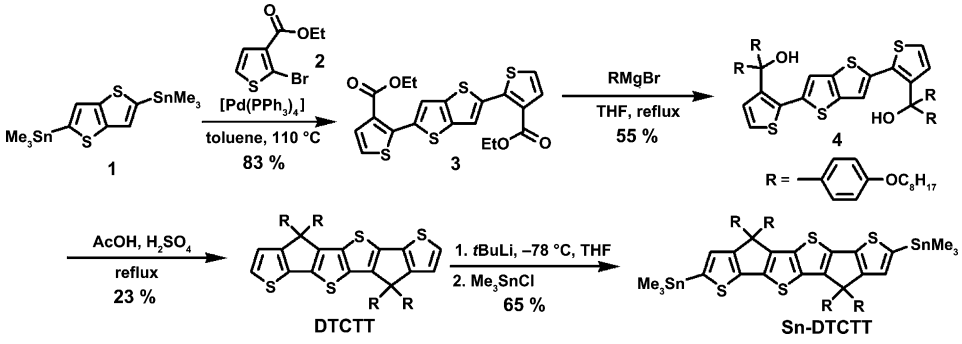

Scheme 3. The synthesis of monomer **Sn-DTCTT**.

Results and Discussion

Synthesis

The synthesis of the **DTCTT** monomer is shown in Scheme 3. 2,5-Bis(trimethylstannyl)thieno[3,2-*b*]thiophene (**1**)[10] was treated with ethyl-2-bromothiophene-3-carboxylate (**2**) by Stille coupling to obtain compound **3**. Double nucleophilic addition of freshly prepared 4-(octyloxy)phenylmagnesium bromide to the ester groups of compound **3** led to the formation of benzylic alcohol **4**, which was subjected to intramolecular annulation through an acid-mediated Friedel–Crafts reaction to furnish the fused nonacyclic arene, **DTCTT**.[11] The Friedel–Crafts cyclization between two adjacent thiophene units was more challenging than for its biphenyl-based analogue, presumably owing to the higher ring-strain. The octyloxy side-chains at the *para* position of the phenyl rings could stabilize the formation of the carbon cation in the intermediate, thus promoting the intramolecular Friedel–Crafts cyclization. **DTCTT** was efficiently lithiated by *tert*-butyllithium followed by quenching with trimethyltin chloride to afford the distannyl **Sn-DTCTT** in moderate yield (65%). The donor (**Sn-DTCTT**) was copolymerized with **TPD**, **BT**, and **PQX** units by Stille coupling polymerization to afford **PDTCTTTPD** (M_n = 18 kDa, PDI = 2.44), **PDTCTTBT** (M_n = 20 kDa, PDI = 1.55), and **PDTCTTPQX** (M_n = 10 kDa, PDI = 1.41), respectively (Scheme 4). All of the polymerization reactions were carried out under microwave-assisted conditions in only 45 min (Table 1). All of the intermediates, monomers, and corresponding copolymers were fully characterized by ^{1}H and ^{13}C NMR spectroscopy (see the Supporting Information). The resulting copolymers showed excellent solubilities in common organic solvents, such as $CHCl_3$, toluene, chlorobenzene, and 1,2-dichlorobenzene.

Thermal Properties

Thermal properties of these polymers were analyzed by differential scanning calorimetry (DSC) and thermal gravimetric analysis (TGA; Table 1). The decomposition temperatures (T_d) of the polymers were in the range 419–427 °C (Figure 1), thus suggesting their sufficient thermal stabilities for OPV applications. From the DSC measurements, neither glass-transition temperatures nor melting points were

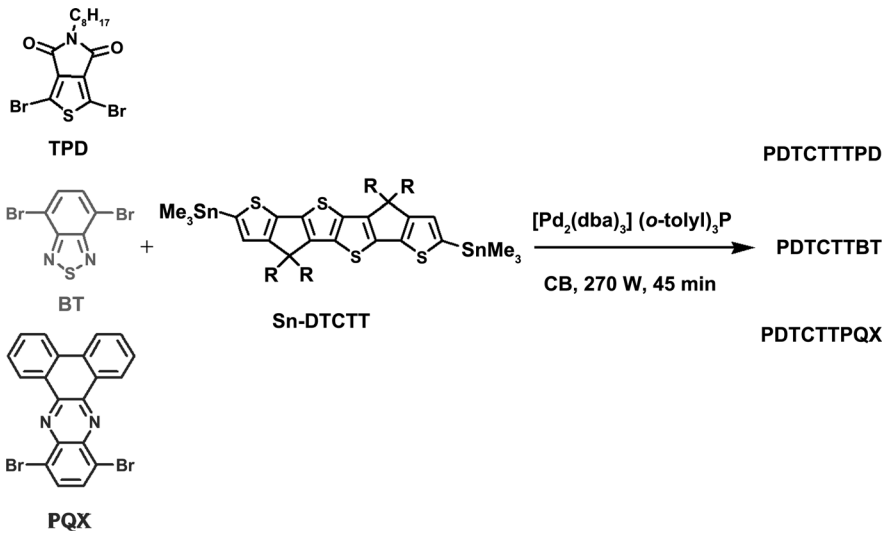

Scheme 4. Stille reactions to afford polymers **PDTCTTTPD**, **PDTCTTBT**, and **PDTCTTPQX**.

Table 1. Molecular weights, polydispersity index and thermal properties of the DTCTT-based polymers.

Copolymer	M_w[a]	M_n[a]	PDI[a]	T_d [°C][b]
PDTCTTTPD	44000	18000	2.44	427
PDTCTTBT	31000	20000	1.55	419
PDTCTTPQX	14400	10200	1.41	420

[a] Molecular weight and polydispersity were determined by gel-permeation chromatography (GPC) in THF. [b] Decomposition temperature (5% weight loss) measured by TGA.

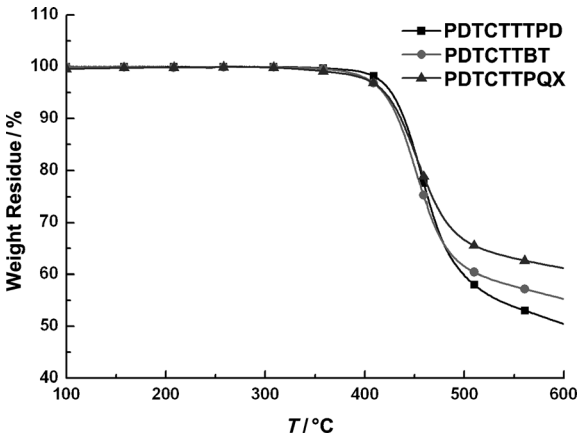

Figure 1. Thermal gravimetric analysis (TGA) measurements of the polymers; ramping rate: 10 °C min^{-1}.

observed for all of the polymers, thus suggesting that these copolymers were amorphous.

Optical Properties

The absorption spectra of these polymers were measured in both dilute $CHCl_3$ (Figure 2) and as thin films (Figure 3); the correlated optical parameters are summarized in Table 2. Copolymers **PDTCTTBT** and **PDTCTTPQX** exhibited two distinct bands in their absorption spectra. One band at shorter wavelengths (400–550 nm) was due to localized π–π* transitions (LT) and the other band at longer wavelengths (550–00 nm) was attributed to intramolecular charge transfer (ICT) between electron-rich donors and electron-deficient acceptors. However, the LT and ICT bands of **PDTCTTTPD** overlapped into a single broad band, which covered the whole visible region (400–750 nm), thereby indicating that the accepting strength of **TPD** was weaker than that of the **BT** and **PQX** units. The absorption spectra

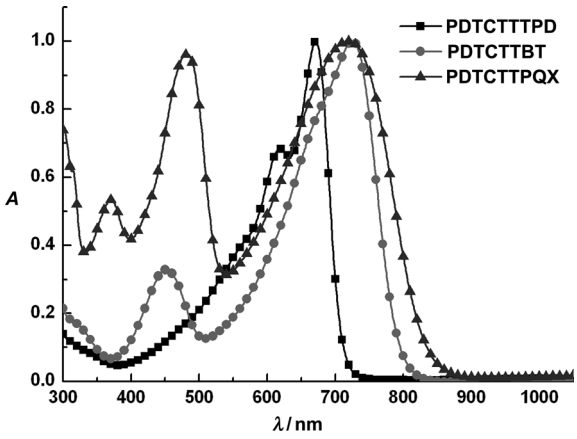

Figure 2. Normalized absorption spectra of the polymers in $CHCl_3$.

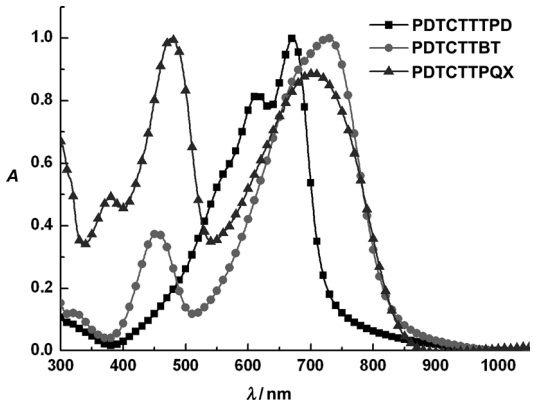

Figure 3. Normalized absorption spectra of the polymers in thin films.

of all of the polymers shifted towards longer wavelengths from the solution state to the solid state, thus indicating that the planar structure of **DTCTT** was capable of inducing stronger interchain π–π interactions. The optical band gaps (E_g^{opt}) deduced from the absorption edges of thin-film spec-

Table 2. Optical properties of the copolymers in the chloroform solution and in the thin film.

Polymer	Solution in $CHCl_3$			Thin film		
	λ_{max} [nm]	λ_{onset} [nm]	E_g^{opt} [eV]	λ_{max} [nm]	λ_{onset} [nm]	E_g^{opt} [eV]
PDTCTTTPD	619, 671	712	1.74	651, 671	721	1.72
PDTCTTBT	451, 714	793	1.56	455, 729	821	1.51
PDTCTTPQX	483, 719	829	1.50	477, 703	838	1.48

tra were in the following order: **PDTCTTPQX** (1.48 eV) < **PDTCTTBT** (1.51 eV) < **PDTCTTTPD** (1.72 eV).

Electrochemical Properties

Cyclic voltammetry (CV) was used to examine the electrochemical properties and evaluate the HOMO and LUMO levels of the polymers (Table 3, Figure 4). All of the polymers showed stable and reversible p-doping and n-doping processes, which are important prerequisites for p-type semiconductor materials. The HOMO energy levels for **PDTCTTTPD**, **PDTCTTBT**, and **PDTCTTPQX** were estimated to be −5.30, −5.08, and −5.04 eV, respectively (Figure 5), which was consistent with the observation that **TPD**-based conjugated polymers generally exhibit lower-lying HOMO energy levels.[12] According to the HOMO–LUMO energy differences, the band-gaps (E_g^{el}; el = electrochemical) obtained from CV measurements were greater than their corresponding optical band-gaps (E_g^{opt}), which was consistent with other literature reports.[13]

Table 3. Electrochemical onset potentials and electronic energy levels of the polymers.

Copolymer	E_{ox}^{onset} [V]	E_{red}^{onset} [V]	HOMO [eV]	$LUMO^{el}$ [eV]	$LUMO^{opt}$[a] [eV]	E_g^{el} [eV]
PDTCTTTPD	0.50	−1.67	−5.30	−3.13	−3.58	2.17
PDTCTTBT	0.28	−1.42	−5.08	−3.38	−3.57	1.70
PDTCTTPQX	0.24	−1.34	−5.04	−3.46	−3.56	1.58

[a] LUMO levels of the polymers were obtained from the equation LUMO = HOMO + E_g^{opt}.

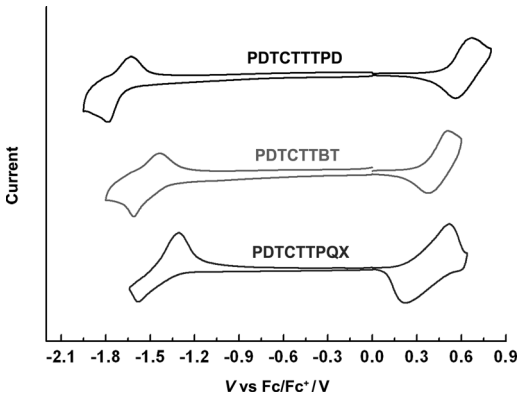

Figure 4. Cyclic voltammograms of the polymers in thin films; scan rate: 80 mV s^{-1}.

Organic Field-Effect Transistors (OFETs) and Photovoltaic Characteristics

The solution-processed OFET devices were fabricated using a bottom-gate, top-contact configuration with evaporated-gold-source/drain-electrodes and an octadecyltrichlorosilane-modified SiO_2-gate dielectric on an n-doped silicon-wafer surface. The

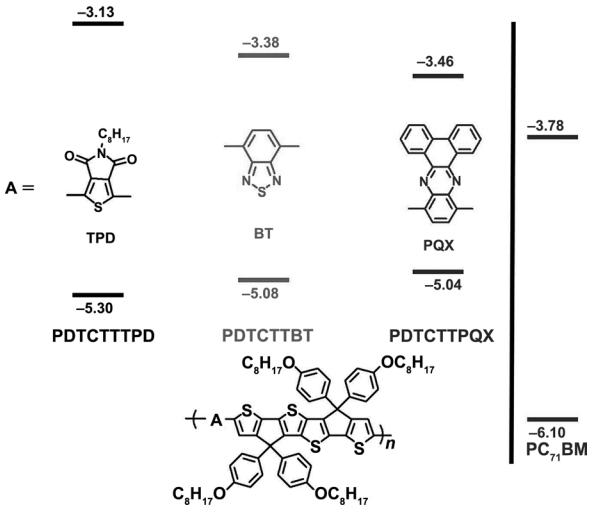

Figure 5. Energy diagram of HOMO–LUMO levels for **DTCTT**-based polymers and $PC_{71}BM$.

output and transfer characteristics of typical devices of **PDTCTTBT** and **PDTCTTPQX** that were annealed at 150 °C are shown in Figure 6, and the corresponding device parameters are shown in Table 4. The hole mobilities of the polymers were calculated from the transport characteristics of the FETs by plotting I_{DS} versus V_{GS}. Polymers **PDTCTTBT** and **PDTCTTPQX** showed impressive saturated field-effect mobilities of 0.053 and 0.017 cm^2 V^{-1} s^{-1} and on/off ratios of 2×10^5 and 3×10^6, respectively. These values are among the highest FET mobilities for amorphous conjugated polymers. Presumably, the rigid and coplanar **DTCTT** unit plays an important role in achieving the high-charge mobility. Nevertheless, **PDTCTTTPD** showed a lower mobility of 2.5×10^{-4} cm^2 V^{-1} s^{-1} with an on/off ratio of 6×10^2.

Bulk heterojunction OPVs were also fabricated on the basis of the ITO/PEDOT:PSS/polymer:$PC_{71}BM$/Ca/Al configuration and their performances were measured under 100 mW cm^{-2} AM 1.5 illumination. The characterization data and the optimal blending ratios of the active layers are summarized in Table 5 and the *J*–*V* curves of these devices are shown in Figure 7. The device based on the **PDTCTTPQX**/$PC_{71}BM$ (1:3, w/w) blend exhibited V_{oc} = 0.62 V, J_{sc} = 7.33 mA cm^{-2}, FF = 42 %, and PCE = 1.91 %. The poorer efficiency may come from the relatively lower molecular weight of **PDTCTTPQX** and the unfavorable

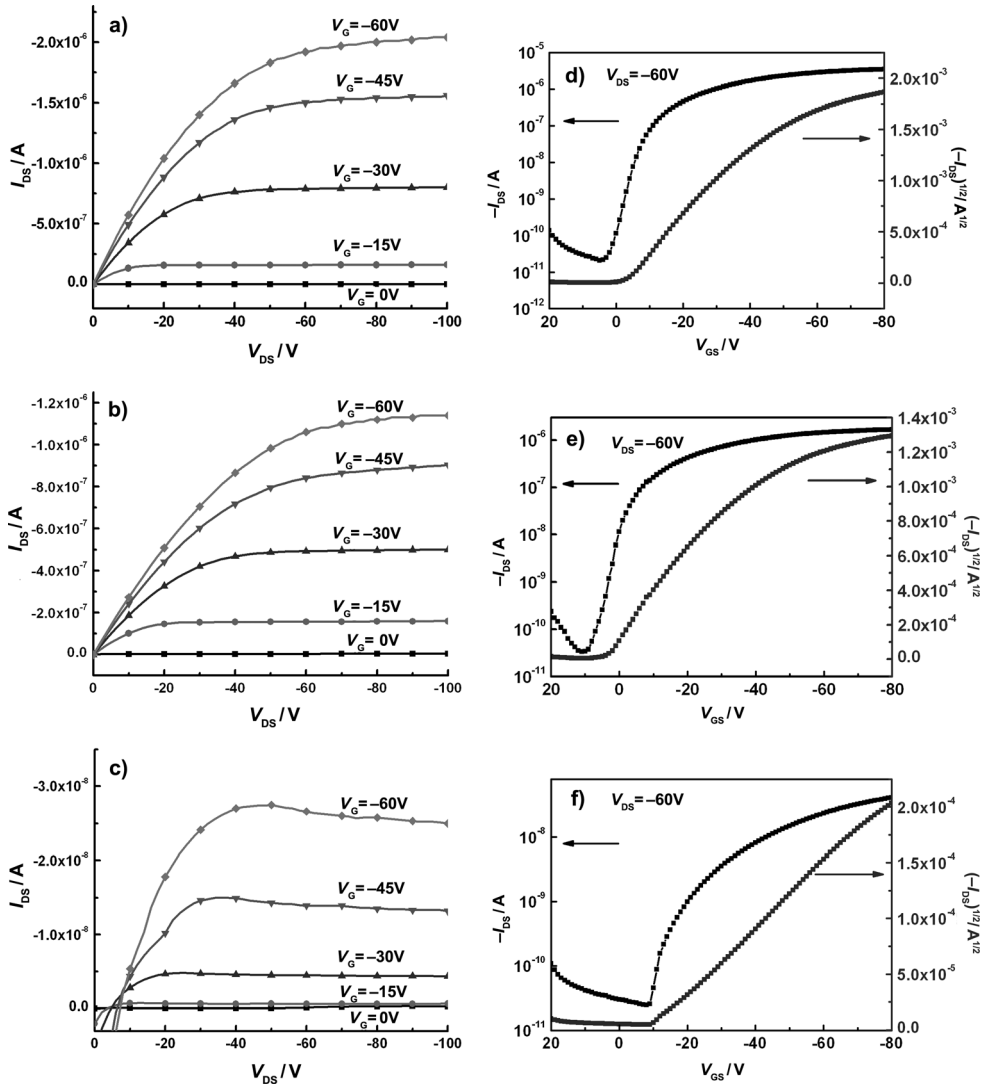

Figure 6. Typical output characteristics of OFETs device of a) **PDTCTTBT**, b) **PDTCTTPQX**, c) **PDTCTTTPD** annealed at 150 °C, and their corresponding transfer characteristics (d–f, respectively).

Table 4. OFET device characteristics.

Copolymer	$T_{annealing}$ [°C]	μ_{hole} [$cm^2V^{-1}s^{-1}$]	I_{on}/I_{off} for holes	$V_{th,\ hole}$ [V]
PDTCTTTPD	150	2.5×10^{-4}	6×10^{2}	0.61
PDTCTTBT	150	5.3×10^{-2}	2×10^{5}	−6.5
PDTCTTPQX	150	1.7×10^{-2}	3×10^{6}	3.45

Table 5. Photovoltaic characteristics.

Copolymer	Ratio of copolymer/$PC_{71}BM$ [wt.%]	Hole mobility [$cm^2V^{-1}s^{-1}$]	V_{oc} [V]	J_{sc} [$mA\,cm^{-2}$]	FF [%]	PCE [%]
PDTCTTTPD	1:2	2.5×10^{-4}	0.72	8.35	43	2.59
PDTCTTBT	1:4	5.3×10^{-2}	0.64	8.03	50	2.57
PDTCTTPQX	1:3	1.7×10^{-2}	0.62	7.33	42	1.91

morphology. The **PDTCTTBT**/$PC_{71}BM$ (1:4, w/w)-based device showed higher J_{sc} and FF values (8.03 $mA\,cm^{-2}$ and 50%, respectively), thereby leading to a PCE of 2.57%. The highest hole mobility for **PDTCTTBT** was responsible for the higher photocurrent of the devices. Furthermore, the device based on the **PDTCTTTPD**/$PC_{71}BM$ (1:2, w/w) blend delivered a V_{oc} value of 0.72 V, a higher J_{sc} value (8.35 $mA\,cm^{-2}$), and an FF value of 43%, thereby producing the highest PCE value of 2.59%. This enhancement of V_{oc} was ascribed to the lowest-lying HOMO energy level of the **PDTCTTTPD** polymer.

Conclusions

We have synthesized a ladder-type hexacyclic **DTCTT** unit, which contained two **CPDT** moieties that were connected through a central thieno[3,2-*b*]thiophene unit. The stannylated **Sn-DTCTT** building block was copolymerized with three electron-deficient acceptors, 1,3-dibromo-5-octyl-thieno[3,4-*c*]pyrrole-4,6-

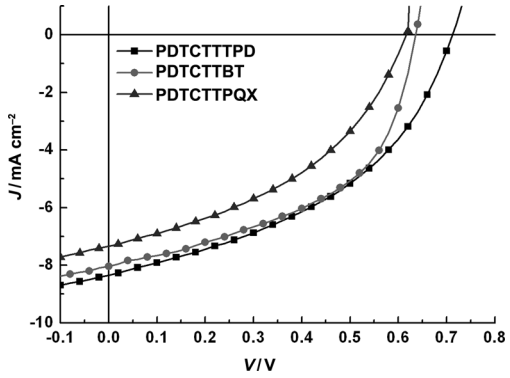

Figure 7. *J–V* characteristics of ITO/PEDOT:PSS/polymer:$PC_{71}BM$/Ca/Al under illumination of AM 1.5, 100 mW cm^{-2}.

dione (**TPD**), 2,7-dibromo-2,1,3-benzothiadiazole (**BT**), and 5,8-dibromo-phenanthrenequinoxaline (**PQX**), by Stille polymerization. The performance of devices based on **PDTCTTTPD**/$PC_{71}BM$ and **PDTCTTPQX**/$PC_{71}BM$ blends exhibited PCE values of 2.59% and 1.91%, respectively. In addition, **PDTCTTBT** not only showed promising hole mobility (0.053 cm^{2}V^{-1}s^{-1}) in bottom-gate OEFTs device, but also exhibited a good PCE value of 2.57% in a polymer solar cell using **PDTCTTBT**/$PC_{71}BM$ (1:4, w/w) as the active layer. This result indicates that the incorporation of coplanar **DTCTT** arenes into conjugated polymers has promise in both OFET and OPV applications.

Experimental Section

General Measurement and Characterization

All chemicals were purchased from Aldrich or Acros and used as received unless otherwise stated. ^{1}H and ^{13}C NMR spectra were measured by using a Varian 300 MHz spectrometer. The molecular weights of the polymers were measured by GPC (Viscotek VE2001GPC), and polystyrene was used as the standard (eluent: THF). Differential scanning calorimeter (DSC) was measured on a TA Q200 Instrument and thermal gravimetric analysis (TGA) was recorded on a Perkin–Elmer Pyris under a nitrogen atmosphere at a heating rate of 10 °C min^{-1}. Absorption spectra were recorded on a HP8453 UV/Vis spectrophotometer. Cyclic voltammetry was conducted on a Bioanalytical Systems Inc. analyzer. A glassy carbon coated with a thin polymer film was used as the working electrode and Ag/AgCl as the reference electrode; electrolyte: 0.1 M tetrabutylammonium hexafluorophosphate ($TBAPF_6$) in MeCN. CV curves were calibrated by using ferrocence as the standard, the HOMO of which was set to −4.8 eV with respect to the zero-vacuum level. The HOMO energy levels were obtained from the equation HOMO = $-(E_{ox}^{onset} - E_{ferrocene}^{onset} + 4.8)$. The LUMO levels of the polymers were obtained from the equation LUMO = $-(E_{red}^{onset} - E_{ferrocene}^{onset} + 4.8)$.

Fabrication and Characterization of the BHJ Device

ITO/glass substrates were ultrasonically cleaned sequentially in detergent, water, acetone, and isopropyl alcohol. Then, the substrates were covered by a 30 nm thick layer of PEDOT:PSS (Clevios P, provided by H. C. Stark) by spin-coating. After annealing in air at 150 °C over 30 min, the samples were cooled to room temperature. The polymers were dissolved in *ortho*-dichlorobenzene (ODCB, 0.47 wt%) and $PC_{71}BM$ (purchased from Nano-C) was added to reach the desired ratio. The solution was then heated at 110 °C and stirred overnight. Prior to deposition, the solution was filtrated through a 0.45 μm filter and the substrates were transferred into a glove box. The photoactive layer was then spin-coated at different speeds to tune its thickness. After drying, the samples were annealed for 15 min. The processing parameters (spin-coating speed, annealing temperature) were as follows: **PDTCTTTPD**/$PC_{71}BM$ (900 rpm; 150 °C), **PDTCTTBT**/$PC_{71}BM$ (800 rpm; 150 °C), **PDTCTTPQX**/$PC_{71}BM$ (600 rpm; 150 °C). The cathode made of calcium (35 nm thick) and aluminum (100 nm thick) was evaporated through a shadow mask under high vacuum ($<10^{-6}$ torr). Each device was constituted of 4 pixels and defined by an active area of 0.04 cm^2. Finally, the devices were encapsulated and *I–V* curves were measured in air.

Electrical Characterization under Illumination

The devices were characterized under 100 mW cm^{-2} AM 1.5 simulated light measurement (Yamashita Denso solar simulator). Current-density-voltage (*J–V*) characteristics of the PSC devices were obtained by a Keithley 2400 SMU. Solar illumination conforming the JIS Class AAA was provided by a SAN-EI 300W solar simulator equipped with an AM 1.5G filter. The light intensity was calibrated with a Hamamatsu S1336–5BK silicon photodiode. The performances presented herein were the average of the 4 pixels of each device.

OFET Fabrication and Characterization

Bottom-gate/top-contact (BG/TC) OFETs were fabricated to investigate the charge-transport properties of the polymers. For the BGTC devices, the semiconductor layers were deposited by spin-coating a 5 mg mL^{-1} polymer solution in ODCB under a N_2 atmosphere onto OTS-treated, n-doped Si wafers that had a 300 nm SiO_2 dielectric layer. The capacitance of the 300 nm SiO_2 gate insulator was 11 nF cm^{-2}. The devices were subsequently annealed for 10 min at 150 °C in a glove box under a N_2 atmosphere. Electrical measurement of the OFET devices was carried out at room temperature in air by using a 4156C, Agilent Technologies. The field-effect mobility was calculated in the saturation regime by using the equation $I_{DS} = (\mu W C_i/2L)(V_G - V_T)^2$, where I_{DS} is the drain-source current, μ is the field-effect mobility, W is the channel width (100 μm), L is the channel length (1 mm), C_i is the capacitance per unit area of the gate dielectric layer (11 nF/cm^2), and V_G is the gate voltage.

*Synthesis of Compound **3***

To a 50 mL round-bottomed flask was added compound **1** (7.30 g, 15.6 mmol), ethyl 2-bromothiophene-3-carboxylate (**2**; 8.10 g, 34.5 mmol), [$Pd(PPh_3)_4$] (0.91 g, 0.78 mmol), and degassed toluene (156 mL). The mixture was heated to reflux under a N_2 atmosphere for 24 h. After removal of toluene under reduced pressure, the residue was purified by column chromatography on silica gel (*n*-hexane /EtOAc, 20:1 v/v) and then recrystallized from THF to give an orange solid (5.48 g, 83%). ^{1}H NMR ($CDCl_3$, 300 MHz): $\delta = 7.67$ (s, 2H), 7.52 (d, $J = 5.4$ Hz, 2H), 7.23 (d, $J = 5.4$ Hz, 2H), 4.32 (q, $J = 7.2$ Hz, 4H), 1.33 ppm (t, $J = 7.2$ Hz, 6H); ^{13}C NMR ([D_8]THF, 75 MHz): $\delta = 163.3$, 143.5, 141.5, 137.4, 131.6, 129.6, 125.7, 122.4, 61.3, 14.6 ppm; MS (EI): *m/z* calcd for $C_{20}H_{16}O_4S_4$: 448.60; found: 448.

*Synthesis of Compound **4***

A Grignard reagent was prepared according to the following procedure. To a suspension of magnesium turnings (1.46 g, 61.0 mmol) and 1,2-dibromoethane (3–4 drops) in dry THF (61 mL) was slowly added 1-bromo-4-(octyloxy)benzene (17.36 g, 61.0 mmol) dropwise and the mixture was stirred for 1 h. To a solution of compound **3** (2.18 g, 4.86 mmol) in dry THF (55 mL) under a N_2 atmosphere was added 4-(octyloxy)benzene-1-magnesium bromide (48.6 mL, 48.6 mmol) dropwise at room temperature. The resulting mixture was heated to reflux for 16 h. The reaction mixture was extracted with EtOAc (3 × 400 mL) and water (150 mL). The combined organic layer was dried over $MgSO_4$. After removal of the solvent under reduced pressure, the residue was purified by column chromatography on silica gel (*n*-hexane /EtOAc, 20:1 v/v) to give a brown oil (3.94 g, 69%). ^{1}H NMR ($CDCl_3$, 300 MHz): $\delta = 7.20$–7.10 (m, 10H), 6.80 (d, $J = 6.9$ Hz, 8H), 6.75 (s, 2H), 6.43 (d, $J = 5.4$ Hz, 2H), 3.94 (t, $J = 6.5$ Hz, 8H), 3.25 (br s, 2H), 1.90–1.70 (m, 8H), 1.50–1.20 (m, 40H),

1.00–0.80 ppm (m, 12H); ^{13}C NMR ($CDCl_3$, 75 MHz): δ = 158.3, 146.2, 139.9, 139.6, 137.0, 131.6, 131.5, 128.7, 123.9, 120.6, 113.7, 80.1, 67.9, 31.8, 29.4, 29.3, 29.2, 26.0, 22.6, 14.1 ppm; MS (FAB): *m*/*z* calcd for $C_{72}H_{92}O_6S_4$: 1181.76; found: 1182.

Synthesis of ***DTCTT***

To a solution of compound **4** (3.35 g, 2.83 mmol) in boiling acetic acid (450 mL) was added a drop of conc. sulfuric acid and the resulting solution was stirred for 3 h at 95 °C. After removal of the acetic acid under reduced pressure, the residue was purified by column chromatography on silica gel (*n*-hexane /EtOAc, 100:1 v/v) to give a yellow oil (0.74 g, 23 %). ^{1}H NMR ($CDCl_3$, 300 MHz): δ = 7.20–7.10 (m, 10H), 7.03 (s, 2H), 6.78 (d, *J* = 8.7 Hz, 8H), 3.88 (t, *J* = 6.6 Hz, 8H), 1.80–1.60 (m, 8H), 1.50–1.10 (m, 40H), 0.95–0.80 ppm (m, 12H); ^{13}C NMR ($CDCl_3$, 75 MHz): δ = 158.2, 157.4, 148.8, 136.8, 136.6, 134.7, 134.4, 128.9, 125.3, 123.0, 122.2, 114.3, 67.8, 61.1, 31.8, 29.3, 29.24, 29.20, 26.0, 22.6, 14.1 ppm; MS (FAB): *m*/*z* calcd for $C_{72}H_{88}O_4S_4$: 1145.73; found: 1145.

Synthesis of Monomer ***Sn-DTCTT***

To a solution of **DTCTT** (1.20 g, 1.05 mmol) in dry THF (31 mL) was added 1.6 M solution of *t*BuLi in *n*-hexane (2.0 mL, 3.14 mmol) dropwise at −78 °C. After stirring at −78 °C for 1 h, a solution of chlorotrimethylstannane in THF (4.2 mL, 1.0 M, 4.19 mmol) was added via syringe. The mixture was quenched with water and extracted with *n*-hexane (3× 200 mL) and water (50 mL). The combined organic layers were dried over $MgSO_4$. After removal of the solvent under reduced pressure, the residue was purified by recrystallizing from THF to give a yellow solid (1.00 g, 65 %). ^{1}H NMR ($CDCl_3$, 300 MHz): δ = 7.16 (d, *J* = 8.7 Hz, 8H), 7.04 (s, 2H), 6.79 (d, *J* = 8.7 Hz, 8H), 3.90 (t, *J* = 6.5 Hz, 8H), 1.80–1.70 (m, 8H), 1.50–1.20 (m, 40H), 1.00–0.80 (m, 12H), 0.36 ppm (s, 18H); ^{13}C NMR ($CDCl_3$, 75 MHz): δ = 159.3, 158.1, 148.7, 142.7, 138.8, 136.7, 134.8, 134.6, 130.4, 129.0, 114.3, 67.9, 60.6, 31.8, 29.32, 29.28, 29.2, 26.1, 22.6, 14.1 ppm; MS (FAB): calcd for $C_{78}H_{104}O_4S_4Sn_2$: 1471.34; found: 1471; elemental analysis (%) calcd for $C_{78}H_{104}O_4S_4Sn_2$: C 63.67, H 7.12; found: C 63.73, H 7.22.

Synthesis of ***PDTCTTTPD***

To a 15 mL round-bottomed flask was added **Sn-DTCTT** (155 mg, 0.105 mmol), 1,3-dibromo-5-octyl-thieno[3,4-*c*]pyrrole-4,6-dione (**TPD**; 44.6 mg, 0.105 mmol), [Pd_2(dba)$_3$] (3.86 mg, 0.0042 mmol; dba = dibenzylidene acetone), tri(*o*-tolyl)phosphine (10.26 mg, 0.032 mmol), and dry chlorobenzene (4.5 mL). The mixture was degassed by bubbling through N_2 gas for 10 min at room temperature. The flask was placed into a microwave reactor and reacted for 45 min at 270 Watt. Then, tributyl(thiophen-2-yl)stannane (19.7 mg, 0.053 mmol) was added and the mixture was reacted for 10 min at 270 Watt. Finally, 2-bromothiophene (9.3 mg, 0.057 mmol) was added and the solution was reacted for 10 min at 270 Watt. Next, the solution was added dropwise into MeOH. The precipitate was collected by filtration and washed by Soxhlet extraction sequentially with acetone and $CHCl_3$ for 3 days. Pd–thiol gel (Silicycle Inc.) and Pd–TAAcOH were added to the $CHCl_3$ solution to remove the residual Pd catalyst and Sn metal. After filtration and removal of the solvent, the polymer was re-dissolved in $CHCl_3$ and added into MeOH to force re-precipitation. The purified polymer was collected by filtration and dried under vacuum for 1 day to give a dark-purple solid (129 mg, 87 %, M_n = 18000, PDI = 2.44). ^{1}H NMR ($CDCl_3$, 300 MHz): δ = 7.60–7.40 (m, 2H), 7.30–7.10 (m, 8H), 7.00–6.70 (m, 8H), 4.10–3.80 (m, 10H), 1.90–1.60 (m, 8H), 1.50–0.95 (m, 55H), 0.90–0.70 ppm (m, 12H).

Synthesis of ***PDTCTTBT***

To a 15 mL round-bottomed flask was added **Sn-DTCTT** (155 mg, 0.105 mmol), 4,7-dibromo-2,1,3-benzothiadiazole (**BT**; 31.0 mg, 0.105 mmol), [Pd_2(dba)$_3$] (3.86 mg, 0.0042 mmol), tri(*o*-tolyl)phosphine (10.26 mg, 0.032 mmol), and dry chlorobenzene (4.5 mL). The mixture was degassed by bubbling through N_2 gas for 10 min at room temperature. The flask was placed into a microwave reactor and reacted for 45 min at 270 Watt. Then, tributyl(thiophen-2-yl)stannane (19.7 mg, 0.053 mmol) was added and the mixture was reacted for 10 min at 270 Watt. Finally, 2-bromothiophene (9.3 mg, 0.057 mmol) was added and the solution was reacted for 10 min at 270 Watt. The solution was added dropwise into MeOH. The precipitate was collected by filtration and washed by Soxhlet extraction sequentially with acetone, *n*-hexane , and $CHCl_3$ for 1 week. Pd–thiol gel (Silicycle Inc.) and Pd–TAAcOH were added to the $CHCl_3$ solution to remove the residual Pd catalyst and Sn metal. After filtration and removal of the solvent, the polymer was re-dissolved in $CHCl_3$ and added into MeOH to force re-precipitation. The purified polymer was collected by filtration and dried under vacuum for 1 day to give a black solid (114 mg, 85 %, M_n = 20000, PDI = 1.55). ^{1}H NMR ($CDCl_3$, 300 MHz): δ = 8.20–8.00 (m, 2H), 7.80–7.60 (m, 1H), 7.30–7.00 (m, 9H), 6.90–6.60 (m, 8H), 4.10–3.70 (m, 8H), 1.90–1.60 (m, 8H), 1.50–1.10 (m, 40H), 1.00–0.80 ppm (m, 12H).

Synthesis of ***PDTCTTPQX***

To a 15 mL round-bottomed flask was added **Sn-DTCTT** (130 mg, 0.088 mmol), 5,8-dibromo-phenanthrenequinoxaline (**PQX**; 38.71 mg, 0.088 mmol), [Pd_2(dba)$_3$] (3.24 mg, 0.0035 mmol), tri(*o*-tolyl)phosphine (8.61 mg, 0.028 mmol), and dry chlorobenzene (3.8 mL). The mixture was degassed by bubbling through N_2 gas for 10 min at room temperature. The flask was placed into a microwave reactor and reacted for 45 min at 270 Watt. Then, tributyl(thiophen-2-yl)stannane (16.5 mg, 0.044 mmol) was added and the mixture was reacted for 10 min at 270 Watt. Finally, 2-bromothiophene (7.78 mg, 0.048 mmol) was added and the mixture was reacted for 10 min at 270 Watt. The solution was added dropwise into MeOH. The precipitate was collected by filtration and washed by Soxhlet extraction sequentially with acetone, *n*-hexane , and $CHCl_3$ for 1 week. Pd–thiol gel (Silicycle Inc.) and Pd–TAAcOH were added to the $CHCl_3$ solution to remove the residual Pd catalyst and Sn metal. After filtration and removal of the solvent, the polymer was re-dissolved in $CHCl_3$ and added into MeOH to force re-precipitation. The purified polymer was collected by filtration and dried under vacuum for 1 day to give a black solid (90.3 mg, 72 %, M_n = 10200, PDI = 1.41). ^{1}H NMR ($CDCl_3$, 300 MHz): δ = 9.60–9.30 (m, 2H), 8.70–8.40 (m, 2H), 8.20–7.60 (m, 8H), 7.50–7.30 (m, 8H), 7.00–6.70 (m, 8H), 4.10–3.70 (m, 8H), 1.85–1.60 (m, 8H), 1.50–1.00 (m, 40H), 0.90–0.70 ppm (m, 12H).

Acknowledgements

We thank the National Science Council and the "ATU Program" of the Ministry of Education, Taiwan, for financial support.

[1] a) G. Yu, J. Gao, J. C. Hummelen, F. Wudl, A. J. Heeger, *Science* **1995**, *270*, 1789–1791; b) S. Günes, H. Neugebauer, N. S. Sariciftci, *Chem. Rev.* **2007**, *107*, 1324–1338; c) B. C. Thompson, J. M. J. Fréchet, *Angew. Chem.* **2008**, *120*, 62–82; *Angew. Chem. Int. Ed.* **2008**, *47*, 58–77; d) Y.-J. Cheng, S.-H. Yang, C.-S. Hsu, *Chem. Rev.* **2009**, *109*, 5868–5923.

[2] a) J. Roncali, *Chem. Rev.* **1997**, *97*, 173–206; b) H. A. M. van Mullekom, J. A. J. M. Vekemans, E. E. Havinga, E. W. Meijer, *Mater. Sci. Eng. R* **2001**, *32*, 1–40; c) J. Chen, Y. Cao, *Acc. Chem. Res.* **2009**, *42*, 1709–1718.

[3] a) Q. Zheng, B. J. Jung, J. Sun, H. E. Katz, *J. Am. Chem. Soc.* **2010**, *132*, 5394–5404; b) J.-S. Wu, Y.-J. Cheng, M. Dubosc, C.-H. Hsieh, C.-Y. Chang, C.-S. Hsu, *Chem. Commun.* **2010**, *46*, 3259–3261; c) Y. Liang, Z. Xu, J. Xia, S.-T. Tsai, Y. Wu, G. Li, C. Ray, L. Yu, *Adv. Mater.* **2010**, *22*, E135-E138; d) L. Huo, J. Hou, S. Zhang, H.-Y. Chen, Y. Yang, *Angew. Chem.* **2010**, *122*, 1542–1545; *Angew. Chem. Int. Ed.* **2010**, *49*, 1500–1503; e) N. Allard, R. B. Aïch, D. Gendron, P.-L. T. Boudreault, C. Tessier, S. Alem, S.-C. Tse, Y. Tao, M. Leclerc, *Macromolecules* **2010**, *43*, 2328–2333; f) N. Blouin, A. Michaud, M. Leclerc, *Adv. Mater.* **2007**, *19*, 2295–2300; g) E. Zhou, M. Nakamura, T. Nishizawa, Y. Zhang, Q. Wei, K. Tajima, C. Yang, K. Hashimoto, *Macromolecules* **2008**, *41*, 8302–8305; h) J. Hou, H.-Y Chen, S. Zhang, G. Li, Y. Yang, *J. Am. Chem. Soc.* **2008**, *130*,

16144–16145; i) Y.-J. Cheng, J.-S. Wu. P.-I. Shih, C.-Y. Chang, P.-C. Jwo, W.-S Kuo, C.-S. Hsu, *Chem. Mater.* **2011**, *23*, 2361–2369.

[4] a) J. Roncali, *Macromol. Rapid Commun.* **2007**, *28*, 1761–1775 and reference therein; b) M. Forster, K. O. Annan, U. Scherf, *Macromolecules* **1999**, *32*, 3159–3162.

[5] a) J. L. Brédas, J. P. Calbert, D. A. da Silva Filho, J. Cornil, *Proc. Natl. Acad. Sci. USA* **2002**, *99*, 5804–5809; b) S. Ando, J.-I. Nishida, H. Tada, Y. Inoue, S. Tokito, Y. Yamashita, *J. Am. Chem. Soc.* **2005**, *127*, 5336–5337; c) N.-S. Baek, S. K. Hau, H.-L. Yip, O. Acton, K.-S. Chen, A. K.-Y. Jen, *Chem. Mater.* **2008**, *20*, 5734–5736; d) Y. Liang, Y. Wu, D. Feng, S.-T. Tsai, H.-J. Son, G. Li, L. Yu, *J. Am. Chem. Soc.* **2009**, *131*, 56–57.

[6] a) P. Coppo, M. L. Turner, *J. Mater. Chem.* **2005**, *15*, 1123–1133; b) P. Coppo, D. C. Cupertino, S. G. Yeates, M. L. Turner, *Macromolecules* **2003**, *36*, 2705–2711.

[7] Z. Zhu, D. Waller, R. Gaudiana, M. Morana, D. Mühlbacher, M. Scharber, C. Brabec, *Macromolecules* **2007**, *40*, 1981–1986.

[8] a) L. Biniek, C. L. Chochos, G. Hadziioannou, N. Leclerc, P. Lévêque, T. Heiser, *Macromol. Rapid Commun.* **2010**, *31*, 651–656; b) L. Biniek, S. Fall, C. L. Chochos, D. V. Anokhin, D. A. Ivanov, N. Leclerc, P. Lévêque, T. Heiser, *Macromolecules* **2010**, *43*, 9779–9786; c) L. Biniek, C. L. Chochos, N. Leclerc, G. Hadziioannou, J. K. Kallitsis, R. Bechara, P. Lévêque, T. Heiser, *J. Mater. Chem.* **2009**, *19*, 4946–4951.

[9] a) L. San Miguel, A. J. Matzger, *Macromolecules* **2007**, *40*, 9233–9237; b) X. Zhang, M. Köhler, A. J. Matzger, *Macromolecules* **2004**, *37*, 6306–6315.

[10] a) L. S. Fuller, B. Iddon, K. A. Smith, *J. Chem. Soc. Perkin Trans. 1* **1997**, 3465–3470; b) M. Sato, A. Asami, G. Maruyama, M. Kosuge, J. Nakayama, S. Kumakura, T. Fujihara, K. Unoura, *J. Organomet. Chem.* **2002**, *654*, 56–65.

[11] H. Bronstein, R. S. Ashraf, Y. Kim, A. J. P. White, T. Anthopoulos, K. Song, D. James, W. Zhang, I. McCulloch, *Macromol. Rapid Commun.* **2011**, *32*, 1664–1668.

[12] a) Y. Zou, A. Najari, P. Berrouard, S. Beaupré, B. R. Aïch, Y. Tao, M. Leclerc, *J. Am. Chem. Soc.* **2010**, *132*, 5330–5331; b) Y. Zhang, S. K. Hau, H.-L. Yip, Y. Sun, O. Acton, A. K.-Y. Jen, *Chem. Mater.* **2010**, *22*, 2696–2698; c) T.-Y. Chu, J. Lu, S. Beaupré, Y. Zhang, J.-R. Pouliot, S. Wakim, J. Zhou, M. Leclerc, Z. Li, J. Ding, Y. Tao, *J. Am. Chem. Soc.* **2011**, *133*, 4250–4253; d) Y. Zhang, J. Zou, H.-L. Yip, Y. Sun, J. A. Davies, K.-S. Chen, O. Acton, A. K.-Y. Jen, *J. Mater. Chem.* **2011**, *21*, 3895–3902.

[13] a) M. M. Wienk, J. M. Kroon, W. J. H. Verhees, J. Knol, J. C. Hummelen, P. A. van Hal, R. A. J. Janssen, *Angew. Chem.* **2003**, *115*, 3493–3497; *Angew. Chem. Int. Ed.* **2003**, *42*, 3371–3375; b) Y. Yao, C. Shi, G. Li, V. Shrotriya, Z. Pei, Y. Yang, *Appl. Phys. Lett.* **2006**, *89*, 153507–153510.

Received: December 2, 2011
Published online: February 6, 2012

